JOURNAL OF GUIDANCE, CONTROL, AND DYNAMICS
Vol. 25, No. 1, January–February 2002

Robust Control of Linearized Poiseuille Flow

Lubomír Baramov,* Owen R. Tutty,† and Eric Rogers‡
University of Southampton, Southampton, England SO17 1BJ, United Kingdom

An approach to feedback control of linearized planar Poiseuille flow using H_∞ control is developed. Surface transpiration is used to control the flow, and point measurements of the wall shear stress are assumed to monitor its state. A high- but finite-dimensional model is obtained via a Galerkin procedure, and this model is approximated by a low-dimensional one using Hankel-optimal model reduction. For the purposes of control design, the flow is modeled as an interconnection of this low-dimensional system and a perturbation, reflecting the uncertainty in the model. The goal of control design is to achieve robust stability, that is, to stabilize any combination of the nominal plant and a feasible perturbation, and to satisfy certain performance requirements. Two different types of surface actuation are considered, harmonic transpiration and a model of a pair of suction/blowing panels. It is found that the latter is more efficient in suppressing disturbances in terms of the control effort required.

Nomenclature

$\boldsymbol{A}, \boldsymbol{B}, \boldsymbol{C}, \boldsymbol{D}$	=	matrices of the finite state-space representation (subscripts may be used to distinguish between different types of states/inputs/outputs)
$a_{mn}(t)$	=	coefficients of a two-dimensional Chebyshev/Fourier expansion
d	=	flow disturbance
$G_{\text{nom}}(s)$	=	nominal transfer function
$G^s(s)$, $G^u(s)$	=	stable/unstable part of $G^{M,N}_{uz}(s)$
$\hat{G}^{sk}(s)$	=	kth-order Hankel approximation of $G^s(s)$
$G_{uy}(s)$, $\boldsymbol{T}_{wz}(s)$	=	transfer function/matrix from the input $u/\boldsymbol{w}$ to the output $y/\boldsymbol{z}$
$G^M_{uz}(s)$	=	transfer function for a single wave number model and Chebyshev order M
$G^{M,N}_{uz}(s)$	=	transfer function for Chebyshev order M and Fourier order N
$\hat{G}_{uz}(s)$	=	low-order approximation of $G_{uz}(s)$
$\boldsymbol{I}, \boldsymbol{0}$	=	identity/zero matrix
j	=	imaginary unit $\sqrt{(-1)}$
$K(s)$	=	controller transfer function
L	=	fundamental channel length
$l(x)$	=	function defining the spatial distribution of blowing/suction
M, N	=	Chebyshev/Fourier expansion orders
$\|\boldsymbol{M}\|$	=	spectral norm of a complex matrix (the largest singular value)
$p(x, y, t)$	=	pressure
$\hat{p}(x, y, t)$	=	deviation of pressure from its base-flow value
$q(t)$	=	function controlling transpiration velocity ($v = -\mathrm{d}l/\mathrm{d}x \cdot q$)
Re	=	Reynolds number
$S(s)$, $T(s)$	=	sensitivity/complementary sensitivity function
s	=	Laplace transform argument
$\|\boldsymbol{T}(s)\|_\infty$	=	H_∞ norm of a stable operator
t	=	time
$U(y)$	=	base flow streamwise velocity
$u(x, y, t)$, $v(x, y, t)$	=	streamwise/cross-channel velocities
$\hat{u}(x, y, t)$, $\hat{v}(x, y, t)$	=	deviations of velocities from the base-flow values
$W(\omega)$	=	perturbation magnitude bound
$\boldsymbol{W}_{i1}$, $\boldsymbol{W}_{i2}$	=	input scales in the control setting
$W_{o1}(s), \ldots, W_{o4}(s)$	=	output weight filters
$\boldsymbol{w}(t)$, $u(t)$	=	external input/control input
$\|\boldsymbol{w}(t)\|_2$	=	L_2 norm of a function $(0, \infty) \to R$
x, y	=	coordinates in streamwise/cross-channel directions
$\boldsymbol{x}$	=	state
$\boldsymbol{z}(t)$, $y(t)$	=	penalized/measurement output
$z(x, y, t)$	=	shear $(\partial\hat{u}/\partial y)$
α_0	=	fundamental wave number
$\Gamma_m(y)$	=	Chebyshev polynomial of order m
γ	=	H_∞ performance index
$\Delta(s)$	=	perturbation transfer function
ω	=	(dimensionless) angular frequency

Superscript

T	=	matrix transposition operator

I. Introduction

RECENTLY flow control has attracted considerable attention in the fluids research community. One of the motivations for this comes from the possibility of reducing drag on a body by preventing or delaying transition from laminar to turbulent flow. The systems dealt with in these problems are, in control terms, very complex, nonlinear, and infinite dimensional, even if the fluid flow is comparatively simple. Plane Poiseuille flow, that is, flow between two infinite parallel plates, is one of the simplest and best understood cases of fluid dynamics. Controlling this flow is, however, still a challenging problem, even if it is assumed that deviations from the steady state are small enough for the governing equations to be linearized. The main problem is obtaining a suitable model that can be used for design of a practically implementable, that is, relatively low-dimensional, controller that would stabilize the flow and satisfy certain performance requirements.

Control of linearized plane Poiseuille flow has been the subject of previous research,[1–5] where in Ref. 1 a simple proportional control using distributed actuation/sensing with arrays of shear sensors and thermoelectric actuators was developed; the goal was to modify the dynamical properties of the flow by heating the fluid and changing its viscosity. Other work[2–4] has used boundary control based on transpiration along one of the walls. In Ref. 2, the mathematical model, that is, two-dimensional linearized Navier–Stokes equations with a controlled boundary condition, was approximated, using a Galerkin procedure, by a first-order, finite-dimensional set of ordinary differential equations. Then, a special harmonically distributed blowing

Presented as Paper 2000-2684 at the AIAA Fluids Conference, Denver, CO, 19–22 June 2000; received 16 November 2000; revision received 8 March 2001; accepted for publication 14 March 2001.

*Research Fellow, Department of Electronics and Computer Science.
†Reader, School of Engineering Sciences.
‡Professor, Department of Electronics and Computer Science.

and suction action was employed such that only one wave number (streamwise Fourier component) is affected. Closed-loop stability was then achieved by a simple integral controller with appropriately designed gain.

The same actuation and sensing was used in Ref. 3, but a more advanced, linear quadratic Gaussian (LQG) controller was proposed. The aim was not only stability but also optimality in the sense of minimizing the expected value of a quadratic cost function, assuming that the flow and sensor disturbances are independent, Gaussian, zero mean white noises. The result was improved performance but also a high-dimensional controller. However, it was shown that the controller dimension can be reduced significantly without loss of stability and degradation of performance. Nevertheless, the model reduction method,[3] was not optimal in the sense of minimizing the reduction error, and this error was not taken into account at the control design stage. In Ref. 5, the approach of Joshi et al.[3] was extended to the multiwave number case where distributed sensing together with actuation was assumed.

The work of Bewley and Liu[4] used H_∞ theory to design a controller for Poiseuille flow for a single wave number only and without model order reduction. The disturbances were assumed to belong to the wide class of continuous bounded energy signals, which is closer to the physical nature of most real disturbances than white noise models. This is the setting of H_∞ control theory,[6] which is now well established, but the approach in Ref. 4 is nonstandard in the sense that the controller design was split into the design of an H_∞-suboptimal state-feedback controller and an H_∞-suboptimal state estimator. However, in the full H_∞-suboptimal approach (see Ref. 6, p. 286), additional conditions are included, which results in a much tighter coupling between the controller and estimator.

In this paper, which is an expanded and revised version of Ref. 7, we will investigate the use of robust control techniques for plane Poiseuille flow. We consider the same flow parameters and point sensing as in previous work,[2,3] but we shall include more than one wave number in our control designs. First, in common with Refs. 2 and 3, the transpiration is harmonic and distributed along the full channel length. In this case the controller can only affect the dynamics of one wave number. However, the dynamics of uncontrolled wave numbers can be excited by disturbances, which, in turn, can degrade closed-loop performance. This is taken into account in design and simulations reported here.

The second form of boundary control has transpiration along short sections of the channel only. This is a model of the type of suction and blowing panels that are currently being considered for application in aerospace systems. In this case, the controller affects an infinite number of wave numbers, but, as shown here, only a small number of them are significant for feedback control. To reduce the model order, we use the Hankel-optimal method (see Ref. 8). Then, the flow is modeled as an interconnection of a low-order nominal system and a perturbation. This perturbation is unknown but is assumed to satisfy a certain frequency-domain bound. This upper bound is not obtained rigorously but estimated from the modeling error relative to very high-order Galerkin approximations and increased by an additional margin. One of the goals of controller design here is to find a controller that guarantees closed-loop stability for any combination of the nominal plant and a feasible uncertainty, that is, makes the closed loop robustly stable. It is a major advantage of H_∞ control theory that it, unlike the LQG approach, can address this issue of model uncertainty directly.

The controllers developed in this paper were simulated in the loop with high-order models. In addition, although the controllers have been designed from data from a single operating point, the controllers have been tested in off-design conditions, for example, at different Reynolds numbers.

II. Mathematical Models

A. Finite Approximations

Here we essentially follow Ref. 2 to obtain a finite-dimensional Poiseuille flow model. The flow in the channel is nondimensionalized using the channel half-height and the centerline velocity. We consider a periodic channel of length L so that $-1 \le y \le 1$ and $-L/2 \le x \le L/2$. Let $p(x, y, t)$ be the pressure, and let $u(x, y, t)$ and $v(x, y, t)$ be the velocities in the direction of the x and y axes, respectively. The steady base flow is given by $p(x, y, t) = -2x/Re$, $u(x, y, t) = 1 - y^2 =: U(y)$, and $v(x, y, t) = 0$, where Re is the Reynolds number. Assume that the quantities $\hat{p}(x, y, t) \equiv p(x, y, t) + 2x/Re$, $\hat{u}(x, y, t) \equiv u(x, y, t) - U(y)$, and $\hat{v}(x, y, t) \equiv v(x, y, t)$ are small so that the flow is governed by the linearized Navier–Stokes equations

$$\frac{\partial \hat{\boldsymbol{u}}}{\partial t} + \boldsymbol{U}_0 \cdot \nabla \hat{\boldsymbol{u}} + \hat{\boldsymbol{u}} \cdot \nabla \boldsymbol{U}_0 = -\nabla \hat{p} + \frac{1}{Re} \nabla^2 \hat{\boldsymbol{u}} \tag{1}$$

$$\nabla \cdot \hat{\boldsymbol{u}} = 0 \tag{2}$$

where $\boldsymbol{U}_0 = (U, 0)$ and $\hat{\boldsymbol{u}} = (\hat{u}, \hat{v})$. The boundary conditions are $\hat{\boldsymbol{u}}(x, 1, t) = \boldsymbol{0}$ and $\hat{\boldsymbol{u}}(x, -1, t) = \{0, -[\mathrm{d}l(x)/\mathrm{d}x]q(t)\}$, where the last condition describes the wall-normal blowing/suction. The function $l(x)$ is assumed to be sufficiently smooth and represents the geometric configuration of the blowing and suction elements, and the function $q(t)$ modifies the blowing/suction according to the control law.

To express the Navier–Stokes equations into the form used in this study, write

$$\hat{\boldsymbol{u}} = \left(\frac{\partial \Phi}{\partial y}, -\frac{\partial \Phi}{\partial x} \right) + q(t) \left(l \frac{\partial f}{\partial y}, -\frac{\partial l}{\partial x} f \right) \tag{3}$$

where $f(y)$ is any smooth function that satisfies $f(-1) = 1$ and

$$f(1) = \left. \frac{\partial f(y)}{\partial y} \right|_{y=-1,1} = 0$$

and Φ is a stream function[2,3] that satisfies the homogeneous boundary conditions $\Phi = \partial\Phi/\partial y = 0$ for $y = \pm 1$. As measurement output, we use the streamwise shear component at a point x_i on the lower wall given by

$$z = \left. \left(\frac{\partial^2 \Phi}{\partial y^2} + q \frac{\partial^2 f}{\partial y^2} l \right) \right|_{y=-1, x=x_i} \tag{4}$$

A finite-series approximation of the function Φ was taken as

$$\Phi(x, y, t) \approx \sum_{n=-N}^{N} \sum_{m=0}^{M+4} a_{mn}(t) \exp(jn\alpha_0 x) \Gamma_m(y) \tag{5}$$

where $\Gamma_m(y)$ are Chebyshev polynomials and $\alpha_0 = 2\pi/L$ is the fundamental wave number.

A Galerkin procedure (for details, see Ref. 9) is now applied to produce a set of $(2N + 1)(M + 1)$ ordinary first-order equations, which can be written as

$$\dot{\boldsymbol{x}}_n = \boldsymbol{A}_n \boldsymbol{x}_n + \boldsymbol{B}_{1n} q + \boldsymbol{B}_{2n} \dot{q} + \boldsymbol{B}_{dn} \boldsymbol{d}_n, \qquad n = -N, \ldots, N \tag{6}$$

where $\boldsymbol{x}_n = [a_{0n} \ \cdots \ a_{Mn}]^T$. Here the $\boldsymbol{d}_n$ represent the flow disturbances whose mathematical description is relevant to the choice of the optimality criterion for the control design. If these disturbances are Gaussian white noises the LQG performance index would be suitable,[3] but here we assume that they are arbitrary functions of bounded energy.

This bounded energy concept will be made precise later and leads naturally to the H_∞ criterion, and although the bounded energy assumption seems to be reasonable physically, our choice of the H_∞ method was motivated also by the fact that it can more easily handle model uncertainties. We shall set $\boldsymbol{B}_{dn} = 10^{-10}\boldsymbol{I}$, which means that the disturbances affect all modes uniformly.

The output approximating shear becomes (depending on the sensor location x_i)

$$z = \sum_{n=-N}^{N} \boldsymbol{C}_n(x_i) \boldsymbol{x}_n + D(x_i) q \tag{7}$$

We also assume that the dynamics of the actuator are described by

$$\dot{\boldsymbol{x}}_p = \boldsymbol{A}_p \boldsymbol{x}_p + \boldsymbol{B}_p u, \qquad q = \boldsymbol{C}_p \boldsymbol{x}_p \tag{8}$$

where u is the control input. The derivative of q is then obtained as

$$\dot{q} = \boldsymbol{C}_p \boldsymbol{A}_p \boldsymbol{x}_p + \boldsymbol{C}_p \boldsymbol{B}_p u \tag{9}$$

and Eqs. (6–9), are a standard set of state-space equations on which to base the analysis.

In this work, the actuator model is defined by $\boldsymbol{A}_p = -0.01, \boldsymbol{B}_p = 1$, and $\boldsymbol{C}_p = 1$, that is, a stable approximation of the integrator used in other work.[2,3] Also, as per Ref. 2, we set $L = 4\pi$ and $Re = 10^4$, and in this case, all matrices $\boldsymbol{A}_n$ for $n \neq \pm 2$ are stable. Matrices $\boldsymbol{A}_2$ and $\boldsymbol{A}_{-2}$ have in total one eigenvalue pair with a small positive real part.

We deal with two cases of boundary control. First, as in Refs. 2 and 3, we take $l(x) = \sin(x)$, where main advantage of this control arrangement is that $\boldsymbol{B}_{1n} = \boldsymbol{B}_{2n} = \boldsymbol{0}$ for all $n \neq \pm 2$. Hence, in feedback stabilization terms, we can deal with only one wave number pair. The second case is when $\mathrm{d}l(x)/\mathrm{d}x$ is a smooth approximation of a pair of rectangular pulses of equal widths and opposite amplitudes, which also guarantees that the transpired fluid has zero total mass flux. The transition between 0 and 1 (and vice versa) takes place over a nonzero length. This interval is divided into four equal subintervals, and on each of these $\mathrm{d}l(x)/\mathrm{d}x$ is a fifth-order polynomial so that continuity of the relevant derivatives is guaranteed. This is a model of a pair of blowing/suction panels. Also this type of control action excites the dynamics of all nonzero wave numbers, which makes the controller design problem more challenging. Here the panels were located at $(-1.8\pi, -1.3\pi)$ and $(\pi, -1.5\pi)$ and the sensor at $x = -\pi$.

B. Low-Order Uncertain Models

From this point onward, we shall deal with transfer function matrix representations of systems. If a (finite-dimensional) linear system has a state-space representation $\dot{\boldsymbol{x}} = \boldsymbol{A}\boldsymbol{x} + \boldsymbol{B}\boldsymbol{u}, \boldsymbol{z} = \boldsymbol{C}\boldsymbol{x} + \boldsymbol{D}\boldsymbol{u}$, the transfer function matrix between the input $\boldsymbol{u}$ and output $\boldsymbol{z}$ vectors is given by $\boldsymbol{G}_{uz}(s) = \boldsymbol{C}(s\boldsymbol{I} - \boldsymbol{A})^{-1}\boldsymbol{B} + \boldsymbol{D}$, where s is the Laplace transform variable.

In the remainder of this section, we deal with the case of one input and one output (and, hence, the transfer function matrix is a scalar). Note also that the disturbance in the problem setup is not relevant to closed-loop stability and, hence, will not be discussed in this section. Also instead of considering a particular $G_{uz}(s)$, we consider the set

$$\{[1 + \Delta(s)]G_{\mathrm{nom}}(s) | \#\text{RHP poles of } G_{\mathrm{nom}} = \#\text{RHP poles of } (1 + \Delta)G_{\mathrm{nom}}, \quad \|\Delta(j\omega)\| < W(\omega) \forall \omega \in \Re\} \tag{10}$$

where $\|\cdot\|$ denotes largest singular value of a complex matrix (or absolute value in the scalar case), $G_{\mathrm{nom}}(s)$ is a low-dimensional nominal system, $\Delta(s)$ is an unknown perturbation (or modeling error), which can be infinite dimensional, and $W(\omega)$ is a weight function. In addition to the frequency bound, $\Delta(s)$ is constrained so that any perturbed system has the same number of unstable, that is, (closed) right half-plane (RHP) poles as $G_{\mathrm{nom}}(s)$. Our aim is to find these $G_{\mathrm{nom}}(s)$ and $W(\omega)$ that subsequently become parameters for robust control design.

It is easy to ensure that the number of unstable poles of G_{uz} and G_{nom} is identical, because there is just one complex pair of unstable poles of $G_{uz}(s)$ whose location is well known,[10] and $G_{\mathrm{nom}}(s)$ can be computed from the state–space equations obtained in the preceding section. The main issue now is the choice of the approximation order. Low orders will result in large modeling errors, hence restricting the achievable performance, whereas high orders yield very complicated controllers that are unsuitable for implementation. However, high- but finite-dimensional systems can be significantly reduced without significant increase of modeling error. Here we use the Hankel optimal reduction method[8] for this key task. We have no rigorous way of estimating $W(\omega)$ such that the set (10) is guaranteed to contain the true G_{uz}. Consequently, we obtain our estimate based on very high-order Galerkin approximation and then allow an additional margin.

We shall consider first the case of harmonically distributed transpiration that affects only the single wave number $n = \pm 2$. The position of the shear sensor is fixed at $x_i = \pi$ as in previous work.[2,3] This was chosen to avoid unstable zeros of $G_{uz}(s)$, which would restrict the achievable performance.

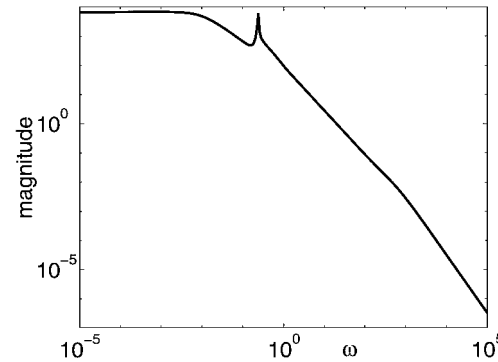

Fig. 1 Magnitude of the single wave number model for $M = 100$.

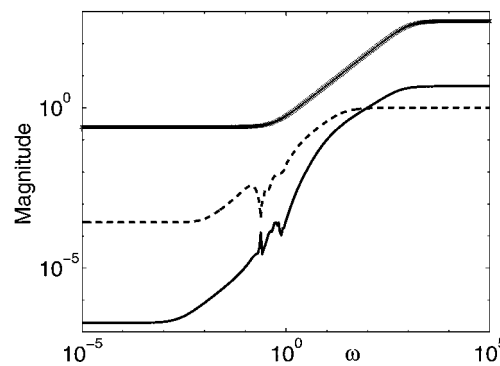

Fig. 2 Comparison of magnitudes of $\delta_{100/40}$ (——), $\hat{\delta}$ (- - -), and $W(\omega)$ (◇).

Consider now approximations for different Chebyshev orders M whose transfer matrices are denoted by $G_{uz}^M(s)$. First we take $G_{uz}^{100}(s)$, which is a system of dimension (including the actuator) $2(M+1)+1 = 203$. Its magnitude plot $|G_{uz}^{100}(j\omega)|$ vs ω is given in Fig. 1 and shows a distinct peak at $\omega \approx 0.23$, which is caused by a pair of unstable poles very close to the imaginary axis. The error relative to G_{uz}^{100} [approximating Δ in Eq. (10)] is $\delta_{100/M}(s) := G_{uz}^{100}(s)/G_{uz}^{M}(s) - 1$, and this error for $M = 40$ is much smaller than 1 for a reasonably broad frequency range (see Fig. 2). For $M = 30$, we could still get acceptable values, whereas for $M = 20$ the model is quite poor and does not even give a sufficiently accurate position of the dominant unstable eigenvalue pair. Using $G_{uz}^{20}(s)$ as $G_{\mathrm{nom}}(s)$ would compromise the achievable performance.

We have established that the error $|\delta_{k/i}(j\omega)|$ is insensitive to k for $k \geq 50$ at frequencies $\omega < 10$. This convinces us that our error estimate is correct for those frequencies. Now consider the approximation $G_{uz}^{40}(s)$, which is a, rather large, rational function of order 83. However, it can be readily reduced using the standard Hankel-optimal model reduction procedure.[8] Its implementation in MATLAB® can be found in the toolbox.[11] This method is applicable to stable transfer matrices only. Therefore, we decompose $G_{uz}^{40}(s)$ as $G_{uz}^{40}(s) = G^s(s) + G^u(s)$, where $G^s(s)$ is the stable part and $G^u(s)$ has all poles in the complex RHP. We apply this reduction technique to $G^s(s)$ to obtain the function $\hat{G}^{sk}(s)$ of order k and also a good estimate (see Ref. 8) of the reduction error $\sup_\omega \|G^s(j\omega) - \hat{G}^{sk}(j\omega)\|$.

In actual fact, $G^s(s)$ can be approximated by a fifth-order function with sufficient precision. Let $\hat{G}_{uz}(s) = \hat{G}^{s5}(s) + G^u(s)$ be our approximation of $G_{uz}^{40}(s)$. Then its error relative to $G_{uz}^{100}(s)$ given by $|\hat{\delta}(j\omega)| = |G_{uz}^{100}(j\omega)/\hat{G}_{uz}(j\omega) - 1|$ (Fig. 2). The moderate increase of modeling error compared to $\delta_{100/40}$ is compensated for by a large reduction in complexity, down from 83 states to 7. Finally, we chose the error weight function of Eq. (10) as $W(\omega) = |0.25(2j\omega + 1)/(0.001j\omega + 1)|$, which places rather conservative upper bounds on $|\hat{\delta}(j\omega)|$ and $|\delta_{100/40}(j\omega)|$ (Fig. 2).

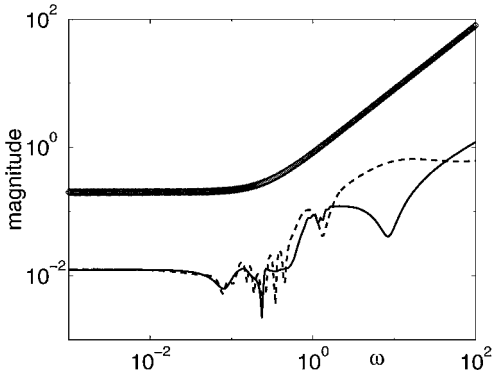

Fig. 3 Magnitudes of $\delta_{120,500/40,6}$ (——), $\hat{\delta}$ (– – –), and $W(\omega)$ (◇).

It was found that the magnitude of the transfer function $G_{uz}(s)$ varies considerably with the position of the sensor, particularly at high frequencies. This naturally raises an issue of robustness with respect to the sensor location. Here we shall assume that we are able to set the position of the sensor with sufficient precision to avoid this problem. Note, however, that, even with a correctly placed sensor, shear responses along the bottom wall may vary significantly if the control signal u has significant high-frequency components.

Now we assume that the transpiration velocity input is proportional to the pair of smoothened rectangular pulses $\mathrm{d}\,l(x)/\mathrm{d}x$ as described in this section. This input excites infinitely many wave numbers, and only using a finite Fourier series approximation introduces an additional modeling error. Let $G_{uz}^{M,N}(s)$ denote the transfer function of the flow when approximated by an a Chebyshev expansion order M and Fourier order N. Examination of the magnitude of $G_{uz}^{M,N}(s)$ showed that, compared to the harmonic case, the frequency response is less sensitive to the position of the sensor. However, here we cannot avoid unstable zeros by choice of x_i, and here we chose $x_i = -\pi$.

Let $\delta_{m,n/i,j}(j\omega) := G_{uz}^{m,n}(j\omega)/G_{uz}^{i,j}(j\omega) - 1$. Then it was found that this quantity is insensitive to n for $m \geq 50$. Based on our earlier discussion, we can assume that $\delta_{m,n/i,j}(j\omega)$ is a good estimate of the modeling error for $\omega < 10$ for $m, n \geq 50$. Figure 3 shows the magnitude plot of $|\delta_{120,500/40,6}(j\omega)|$.

The transfer function $G_{uz}^{40,6}(s)$ is, therefore, a good candidate for the nominal function $G_{\mathrm{nom}}(s)$, but for the fact that its order is 534. Applying the Hankel-optimal reduction procedure, however, gives an approximation $\hat{G}_{uz}(s)$ of order 14, whose relative error with respect to $G_{uz}^{120,500}(s)$ is denoted by $\hat{\delta}(s)$ (Fig. 3 plots both this quantity and its magnitude). Hence the Hankel-optimal reduction gives a much simpler model without significantly increasing the modeling error. Finally, we choose the error bound as $W(\omega) = |0.2(4j\omega + 1)/(0.001j\omega + 1)|$, allowing a generous margin for additional high-frequency modeling errors.

III. Control of Poiseuille Flow

A. Control Problem Formulation

We now formulate a flow control problem in the H_∞ framework where we give only the essential background results; for a detailed treatment of H_∞ control theory see, for example, Ref. 6. Once this problem is formulated, its solution is straightforward, and a controller can be computed using widely available software packages, for example, a MATLAB toolbox.[11]

Consider the standard feedback configuration that consists of generalized controlled plant $\boldsymbol{P}$ described by its transfer matrix written in the form

$$\begin{bmatrix} \boldsymbol{z}(s) \\ \boldsymbol{y}(s) \end{bmatrix} = \boldsymbol{P}(s) \begin{bmatrix} \boldsymbol{w}(s) \\ \boldsymbol{u}(s) \end{bmatrix}, \qquad \boldsymbol{P}(s) = \begin{bmatrix} \boldsymbol{P}_{wz}(s) & \boldsymbol{P}_{uz}(s) \\ \boldsymbol{P}_{wy}(s) & \boldsymbol{P}_{uy}(s) \end{bmatrix}$$

with the inputs $\boldsymbol{w}$ (external inputs, e.g., disturbances) and $\boldsymbol{u}$ (controls) and the outputs $\boldsymbol{z}$ (penalized outputs) and $\boldsymbol{y}$ (measurements). By assumption, $\boldsymbol{w} \in \boldsymbol{L}_2(\boldsymbol{0}, \infty)$, that is the function space with a norm defined as

$$\|\boldsymbol{w}\|_2 := \left[\int_0^\infty \boldsymbol{w}(t)^T \boldsymbol{w}(t)\, \mathrm{d}t \right]^{\frac{1}{2}} < \infty$$

This is referred to as the square root of the generalized energy of the signal $\boldsymbol{w}$. The transfer matrix $\boldsymbol{T}_{wz}(s)$ of the feedback system under the control law $\boldsymbol{u} = \boldsymbol{K}\boldsymbol{y}$ is given by (omitting the argument)

$$\boldsymbol{T}_{wz} = \boldsymbol{P}_{wz} + \boldsymbol{P}_{uz}\boldsymbol{K}(\boldsymbol{I} - \boldsymbol{P}_{uy}\boldsymbol{K})^{-1}\boldsymbol{P}_{wy} \tag{11}$$

The closed-loop performance index is measured in terms of the so-called ∞ norm, where if we assume that $\boldsymbol{T}_{wz}$ is a stable transfer matrix, then

$$\|\boldsymbol{T}_{wz}(s)\|_\infty := \operatorname*{ess\,sup}_{\omega > 0} \|\boldsymbol{T}_{wz}(j\omega)\| \tag{12}$$

An important property of this operator norm is that it is induced from the 2 norm,

$$\|\boldsymbol{T}_{wz}\|_\infty = \sup_{w \in L_2(0,\infty)} \|z\|_2 / \|\boldsymbol{w}\|_2 \tag{13}$$

The objective of control design is to find a controller $\boldsymbol{K}$ such that the closed loop is internally stable, which means that all states of the plant and the controller asymptotically converge to 0 in the absence of external inputs and $\|\boldsymbol{T}_{wz}\|_\infty$ is as small as possible. However, this optimization problem is difficult to solve; instead, we solve a feasibility problem of finding a stabilizing controller $\boldsymbol{K}$ such that $\|\boldsymbol{T}_{wz}\|_\infty < \gamma$, where γ is a positive constant. Then, we search for the smallest γ for which this feasibility problem has a solution. It follows from Eq. (13) that γ^2 is the maximum disturbance-to-optimized-output energy ratio.

One of the main reasons for using the H_∞ norm is that it can be used in a tight robust-stability condition. Consider the feedback system of Fig. 4. The closed-loop transfer function matrix from $\boldsymbol{w}$ to $\boldsymbol{z}$ in the nominal case, that is, $\Delta = 0$ is given by

$$\boldsymbol{T} = (\boldsymbol{I} - \boldsymbol{G}_{\mathrm{nom}}\boldsymbol{K})^{-1}\boldsymbol{G}_{\mathrm{nom}}\boldsymbol{K} \tag{14}$$

and is called complementary sensitivity function in the control literature. Assume that this matrix is stable. Then, the system in Fig. 4 is stable for any $\boldsymbol{G}_{uz}$ from the set (10) if and only if, for all ω, $\|\boldsymbol{T}(j\omega)\|_\infty < 1/W(\omega)$. Suppose also that $\boldsymbol{W}_{o2}(\boldsymbol{s})$ is a stable transfer function matrix with a stable inverse and $\|\boldsymbol{W}_{o2}(j\omega)\| \geq W(\omega)$. Then it follows from properties of the H_∞ norm that this robust stability condition is satisfied if $\|\boldsymbol{W}_{o2}(s)\boldsymbol{T}(s)\|_\infty < 1$.

Now we formulate our control problem in the H_∞ framework. Let our low-order approximation of the flow be given by transfer function matrix $\hat{\boldsymbol{G}}(s) = [\hat{\boldsymbol{G}}_{dz}(s)\ \ \hat{G}_{uz}(s)]$ obtained by the procedure described in the preceding section, where here we have applied model order reduction with disturbances included. [Note that in this specific case $\hat{G}_{uz}(s)$ is a scalar and so are $K(s)$ and $T(s)$.] This is justified by the very small scale of $\boldsymbol{B}_{dn}$ in Eq. (6), and hence, the resulting reduction errors are essentially the same as before. The low-order approximation of $\boldsymbol{G}_{dz}(s)$ is much less accurate than that of $G_{uz}(s)$, but this cannot affect stability.

As was already noted, the unstable part was extracted from the model during the order reduction process. Also only the stable part was approximated by a low-order model. The unstable part here, that is, $G^u(s)$, is known fairly precisely and is, in fact, a generator of slowly growing oscillations of $\omega \approx 0.23$. As a dominant part of the model, it will receive special attention during the design process where its two states, denoted by ξ, will be regarded as a penalized output.

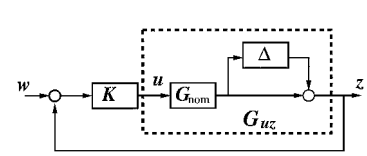

Fig. 4 Simple feedback loop.

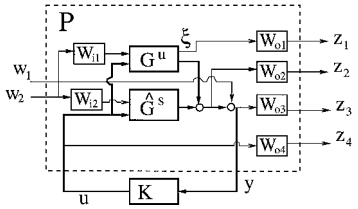

Fig. 5 Flow control in the H_∞ framework.

The transfer function matrix of the generalized plant is now taken to be (Fig. 5)

$$\boldsymbol{P}_N = \left[\begin{array}{cc|c} \mathbf{0} & W_{o1}\boldsymbol{G}_{d\xi}\boldsymbol{W}_{i1} & W_{o1}G^u_{u\xi} \\ \mathbf{0} & W_{o2}\tilde{\boldsymbol{G}}_{dz} & W_{o2}\hat{G}_{uz} \\ W_{o3} & W_{o3}\tilde{\boldsymbol{G}}_{dz} & W_{o3}\hat{G}_{uz} \\ \mathbf{0} & \mathbf{0} & W_{o4} \\ \hline 1 & \tilde{\boldsymbol{G}}_{dz} & \hat{G}_{uz} \end{array}\right] \tag{15}$$

where $\tilde{\boldsymbol{G}}_{dz} = \boldsymbol{G}^u_{dz}\boldsymbol{W}_{i1} + \hat{\boldsymbol{G}}^s_{dz}\boldsymbol{W}_{i2}$. The scalars $W_{o1}, \ldots, W_{o4}$ are either stable transfer functions with stable inverses or constants; if nonconstant, they introduce frequency-dependent weighting into our criterion, which is necessary to find tradeoffs between various conflicting design requirements.

The function $W_{o3}(s)$ weights the perturbed shear output measured by the sensor and the closed-loop transfer function from disturbance w_1 to this output and is the so-called sensitivity function, denoted by $S(s)$. Because w_1 models the effects of uncertain dynamics, we naturally want the magnitude of this transfer function to be as low as possible over a wide frequency range. However, the achievable frequency range is restricted by robustness requirements and also structural limitations, for example, unstable zeros.[6] Assuming that γ is the performance index achieved, the sensitivity function is bounded by $\|S(j\omega)\| \le |W_{o3}(j\omega)^{-1}T_{w_1z_3}(j\omega)| \le \gamma|W_{o3}(j\omega)^{-1}|$. Hence, $W_{o3}(s)$ is typically a low-pass filter.

The filter $W_{o2}(s)$ weights the nominal shear output. The closed-loop transfer matrix from disturbance w_1 to this shear is exactly the mixed sensitivity function $T(s)$ of Eq. (14). We choose $|W_{o2}(j\omega)| \ge W(\omega)$, where $W(\omega)$ is the error bound of Eq. (10). Then, the robust stability condition is satisfied if $\|T_{w_1z_2}(s)\|_\infty < 1$. This is automatically satisfied if (but not only if) $\gamma \le 1$. The weight W_{o4} is usually chosen as a high-pass filter to suppress the high-frequency components of the control input that restricts acceleration of the transpired fluid. Also, at high frequencies, the shear response may vary dramatically along the wall. If these components are present in the control signal, they could result in time responses with high peaks at locations where shear is not measured.

If the remaining weights $\boldsymbol{W}_{i1}$, $\boldsymbol{W}_{i2}$, and W_{o1} are zero, then we have the classical mixed sensitivity problem.[6] This formulation, although useful in many applications, cannot handle effectively flow disturbances $\boldsymbol{d}$ as well as nonzero initial conditions. For instance, the near $j\omega$-axis poles of $G^u(s)$ would be shifted just into the stable domain, but they would have very poor damping. This means that the whole flow would contain lightly damped oscillations with $\omega \approx 0.23$, which may be canceled only at the sensor location. Improved damping can be achieved here by better choice of the weight W_{o1}. The matrices $\boldsymbol{W}_{i1}$, $\boldsymbol{W}_{i2}$ could be used to reflect a priori knowledge of (frequency-dependent) disturbance properties. However, here we only use these matrices to introduce constant scaling.

Checking the existence of an H_∞ controller requires, under mild conditions,[6] solvability of two algebraic Riccati equations, where their solutions have to satisfy a coupling condition. Based on these solutions, the state-space form of a feasible controller can be computed that is of the same order as the plant (including weighting filters). The general form of the equations for an H_∞ controller can be found in Ref. 6, pp. 288–293. We note that these equations, which were used in this work, are different from those given in other work.[4] To compute the optimal performance index γ and the controller, we use the MATLAB routine hinfsyn of Balas et al.[11]

B. Results: Harmonic Transpiration Case

We undertake an H_∞ control design and compare its responses (both frequency and time domain) with those based on the LQG design with prescribed degree of stability reported elsewhere.[3] For time-domain simulations, we chose initial conditions responses, for simplicity and comparison with Ref. 3, although H_∞ control design, unlike LQG designs, does not optimize these responses.

The control configuration is shown in Fig. 5. The parameters were chosen in conjunction with the guidelines outlined in the preceding subsection after several trial-and-error iterations to find a compromise between various conflicting requirements. We chose $\boldsymbol{W}_{i1} = 10^3\boldsymbol{I}$, $\boldsymbol{W}_{i2} = \boldsymbol{I}$, and

$$W_{o1} = 10^5, \qquad W_{o2} = \frac{0.35(2s+1)}{(0.001s+1)}$$

$$W_{o3} = \frac{3000(s+1)^2}{(100s+1)^2}, \qquad W_{o4} = 0.1 \tag{16}$$

The disturbance-input weights $\boldsymbol{W}_{i1}$ and $\boldsymbol{W}_{i2}$ are set to constant matrices because the disturbance spectra are not known and we emphasized the disturbances exciting the unstable part of the flow.

The weight W_{o1} of the state ξ of the unstable part was set to 10^5. It was found that for lower values it is not effective in damping the oscillations and that higher values cause performance degradation. Our choice of the output filter $W_{o2}(s)$ satisfies the robustness condition rather conservatively: We have $|W_{o2}(j\omega)| = 1.4W(\omega)$, which means we are leaving more room for larger modeling errors, or, alternatively, for additional finite-energy disturbances.

The output weight $W_{o3}(s)$ is a second-order, low-pass filter that should force a low shear output over the widest possible frequency range. For simplicity, control weight W_{o4} was taken as a constant. The resulting performance index is $\gamma \approx 0.88$ and the controller $K(s)$ is of order 10.

The simulation setting is as follows. We set the Chebyshev order $M = 40$ and for each wave number $i\alpha_0$, $i = 0, \ldots, 5$ we chose, as a random initial condition, $\boldsymbol{x}_i(0)$ set equal to the MATLAB term 1e−4/(i + 1)^2 ∗ rand(82, 1). To obtain repeatable results, the random number generator was first initialized by the command rand ('state', 0).

The controller and actuator were initialized to 0, and the responses were generated using the MATLAB function trsp for linear system responses.[11] Shear plots measured at $x = x_i = \pi$ are given in Fig. 6. Both H_∞ and LQG controllers do a good job of fast shear reduction. Also, the LQG response settles faster than the H_∞ one, which is slower and also contains some slowly damped oscillations, which are, however, negligible compared to the disturbance size.

Figure 7 shows the blowing/suction responses, and it is clear that both controllers respond very quickly, but the initial response of the LQG controller has a peak that is almost double that of the H_∞ controller. Hence, the LQG controller is much more demanding on actuator speed. In the longer term, both controller responses are very

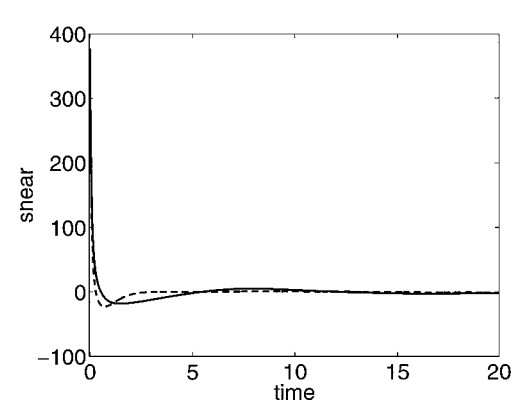

Fig. 6 Shear responses at $x = \pi$: H_∞ controller (——), and LQG controller (– – –).

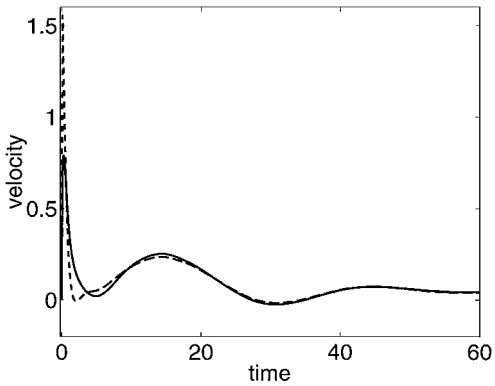

Fig. 7 Blowing/suction responses: H_∞ controller (——), and LQG controller (– – –).

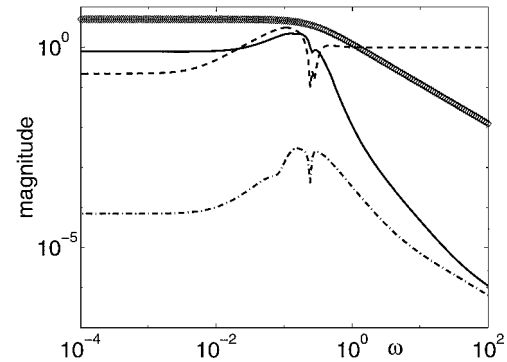

Fig. 8 Magnitudes: sensitivity (– – –), complementary sensitivity (——), control (–·–·–), and $W(\omega)^{-1}$ (◇).

similar. Figure 7 also shows that the whole feedback system needs a much longer time to settle than Fig. 6 may suggest.

Another key issue is shear responses at locations other than $x = x_i = \pi$, which are not directly penalized by either design. For example at $x = \pi/2$, the H_∞ response jumped from its initial value of about 400 to -100 in almost no time, and the whole response needed a much longer time to settle than at $x = \pi$. The LQG response had a much greater overshoot (to -400). This feature is explained by that (1) the frequency range of the LQG control signal is considerably wider than that of the H_∞ one and (2) at high frequencies the control-to-shear responses are very sensitive to x. Examination of the magnitudes of the transfer functions $T_{w_1 z}$ (equal to the mixed sensitivity function) for both controllers and the robustness constraint $W(\omega)^{-1}$ showed that the LQG controller came much closer to the constraint than its H_∞ counterpart and is, therefore, more vulnerable to modeling errors.

Finally, the stability of this closed loop was tested for Reynolds numbers from 5×10^3 to 10^5 in increments of 1000. The closed loop was stable for the whole set.

C. Results: Discrete Transpiration Case

Here we shall deal with H_∞ control of the channel flow model with a pair of blowing/suction panels. As outlined in Sec. II, robustness requirements here are stricter than in the harmonic case. Also, the plant has one unstable zero, which restricts the frequency range in which the sensitivity function can be made small without making it excessively large elsewhere. This means that, in the time domain, the responses may be relatively slow and oscillatory.

The shear sensor position is $x_i = -\pi$. The design parameters are as follows: $W_{o1} = 1.5 \times 10^5$,

$$W_{o2} = \frac{0.26(2s^2 + 4s + 1)}{(0.001s + 1)^2}, \qquad W_{o3} = \frac{10(4s + 1)}{200s + 1},$$

$$W_{o4} = \frac{200(2s + 1)}{0.001s + 1} \tag{17}$$

The input scale matrix $\boldsymbol{W}_{i2}$ was chosen to be zero, that is, so that the disturbance component that affects the stable eigenspace is ignored and the component disturbing the unstable eigenspace is weighted by $\boldsymbol{W}_{i1} = 10^3$. The output weight W_{o2} is higher than the perturbation bound $W(\omega)$. The other design parameters were chosen after several trial-and-error iteration steps to give a controller K, which results in the closed-loop H_∞ norm with value less than $\gamma \approx 80$.

Figure 8 gives the closed-loop frequency responses and shows that the loop is robustly stable. Also, it can be seen that the control function magnitude is small at very high, and very low frequencies, that is, where the shear is highly sensitive to x.

For the simulation studies, we considered a flow model with $M = 40$ and $N = 10$, and hence, the state-space dimension of the plant simulation model is 863. The controller has 18 states, and the initial condition was chosen as in Sec. II.B. Wave numbers $n\alpha_0$, $n = \pm 6, \ldots, \pm 10$, together with actuator and controller, are initialized to zero and the responses were computed using the standard ode45 solver from MATLAB.

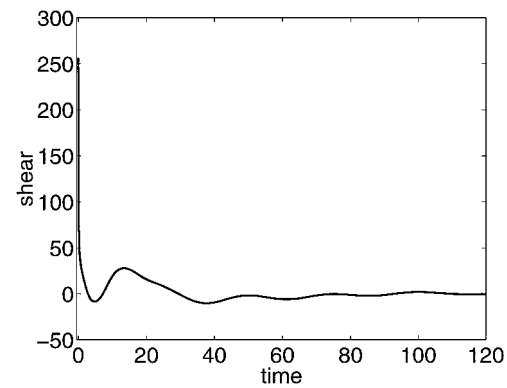

Fig. 9 Shear responses at $x = x_i = -\pi$.

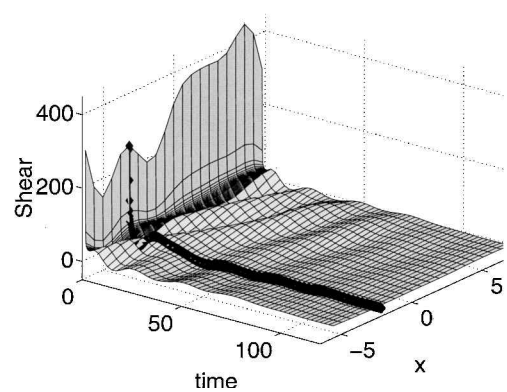

Fig. 10 Shear responses along the wall: diamonds mark the path for $x = x_i$.

Figure 9 shows the response of the measured shear and Fig. 10 shows shear responses along the wall. In Fig. 9, we see that the shear drops very quickly from a large initial value of about 250. This is followed by some slowly damped oscillations that are hard to suppress due to the presence of unstable zeros in the flow model. Nevertheless, their amplitude is small compared to the initial value. Figure 11 shows that the transpiration velocity has a peak significantly lower than in the previous case of harmonic actuation. This also holds for its rate of change around $t = 0$ (Fig. 7). As a consequence, the shear is attenuated very uniformly along the bottom wall (Fig. 10). Notice also in Fig. 11 that the control signal approaches zero very slowly. This is due to the contribution of the zero wave number, which is uncontrollable and contains very slow modes.

Stability of the closed loop was also tested for a range of Reynolds numbers. The highest Reynolds number for which the closed loop is still stable lies between 1.5×10^4 and 1.6×10^4.

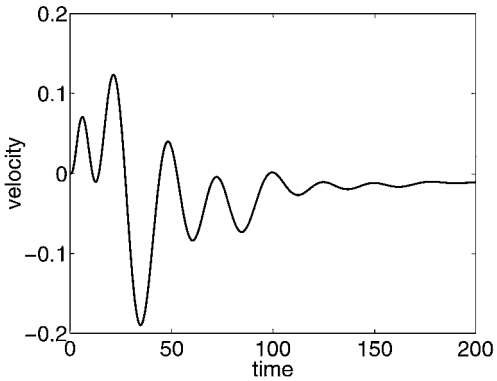

Fig. 11 Blowing/suction responses.

IV. Conclusions

We have investigated an approach to low-dimensional robust control of plane Poiseuille flow. There are several important contributions in the work reported. The first of these is controlling simultaneously (but not independently) multiple wave number dynamics. To achieve this, we had to use an advanced method of model reduction to reduce model complexity significantly. Second, the flow was modeled as an interconnection of a low-dimensional nominal system and an uncertainty. This uncertainty was fully accounted for in controller design, thus making the controller truly robust with respect to modeling uncertainties. Third, frequency-domain analysis and frequency weighting were used in a flow control context.

Finally, different forms of surface transpiration have been considered. This includes a new model of surface transpiration that is a representation of a pair of blowing/suction panels. This is a much simpler actuator configuration than the harmonic one, but it does, however, introduce much stricter performance limitations (due, for example, to larger modeling error and an unstable zero). Against this, however, it requires less control effort (in terms of transpiration velocity magnitudes) than the harmonic arrangement.

The extension of this work to the three-dimensional case is currently under investigation.

References

[1]Hu, H. H., and Bau., H. H., "Feedback Control to Delay or Advance Linear Loss of Stability in Planar Poiseuille Flow," *Proceedings of the Royal Society of Lodon, Series A: Mathematical and Physical Sciences*, Vol. 447, No. 1, 1994, pp. 299–312.

[2]Joshi, S. S., Speyer, J. L., and Kim, J., "A System Theory Approach to the Feedback Stabilization of Infinitesimal and Finite-Amplitude Disturbances in Plane Poiseuille Flow," *Journal of Fluid Mechanics*, Vol. 332, 1997, pp. 157–184.

[3]Joshi, S. S., Speyer, J. L., and Kim, J., "Finite Dimensional Optimal Control of Poiseuille Flow," *Journal of Guidance, Control, and Dynamics*, Vol. 22, No. 2, 1999, pp.340–348.

[4]Bewley, T. R., and Liu, S., "Optimal and Robust Control and Estimation of Linear Paths to Transition," *Journal of Fluid Mechanics*, Vol. 365, 1998, pp. 305–349.

[5]Cortelezzi, L., Speyer, J. L., Lee, K. H., and Kim, J., "Robust Reduced-Order Control of Turbulent Channel Flows via Distributed Sensors and Actuators," *Proceedings of the 37th IEEE Conference on Decision and Control*, Inst. of Electrical and Electronics Engineers, New York, 1998, pp. 1906–1911.

[6]Zhou, K., and Doyle, J. C., *Essentials of Robust Control*, Prentice–Hall, Upper Saddle River, NJ, 1998, pp. 269–300.

[7]Baramov, L., Tutty, O. R., and Rogers, E., "Robust Control of Plane Poiseuille Flow," AIAA Paper 2000-2684, July 2000.

[8]Glover, K., "All Optimal Hankel-Norm Approximations of Linear Multivariable Systems and Their L_∞-Error Bounds," *International Journal of Control*, Vol. 39, No. 6, 1984, pp. 1115–1193.

[9]Canuto, C., Hussaini, M. Y., Quarteroni, A., and Zang, T. A., *Spectral Methods in Fluid Dynamics*, Springer, New York, 1988, pp. 76–182.

[10]Orszag, S. A., "Accurate Solution of the Orr–Sommerfeld Equations," *Journal of Fluid Mechanics*, Vol. 50, 1971, pp. 689–703.

[11]Balas, G. J., Doyle, J. C., Glover, K., Packard, A., and Smith, R., "μ-Analysis and Synthesis Toolbox for Use with MATLAB," User's Guide Ver. 3, Mathworks, Natick, MA, 1998.